Time-Frequency Integration of Variable-Bandwidth Signals and Supplementary Data Packets

Piotr Augustyniak

***Abstract*—**Integration of multimodal measurement signals is necessary for extending the experiment scope, for avoiding accidental data or synchronization loss or for building authorization-dependent data supplement. Instead of signal modulation or packet transmission widely used in such cases, we propose using of efficient watermarking technique based on the bandgap occasionally appearing between the instantaneous bandwidth of the signal and the Nyquist frequency.

Usage of the method requires anticipating studies of the carrier (i.e. main signal) to determine band limits and a confident detection method of its components. Resulting statistics lead to a signal-specific standardized instantaneous bandwidth function.

The method starts with detection of signal components, estimating the expected local bandwidth and measuring of noise properties in the bandgap. The supplementary data are tailored and packetized as so mimic the noise, therefore are not interfering with the carrier message and not conspicuous for an unauthorized reader. Finally an individual description of each packet is made and encoded with optional encryption. As long as the total data streams volume does not excess the channel throughput, the proposed integrating uses the carrier's original transmission channel (with no carrier delay) and data storage structures.

The research was showcased by three applications of watermarking the ECG signal for its best methods for automatic components detection, best knowledge on physiological backgrounds and best documented annotated databases of reference records. Nevertheless, the results of our research will be applicable for any digital measurement series (signals) recorded in biology and industry in which the instantaneous bandwidth could be estimated.

***Keywords*—** time-frequency steganography, variable bandwidth, multimodal measurements, biosignal watermarking.

I. Introduction

FAST development of data interpretation methods requires constant evolution of measurement infrastructure. This is partially faced by development of new sensors and sensing methods, but yet rarely supported by recording hardware and software. Additionally, backward compatibility of digital records is usually in question when adding supplementary structures to the storage format.

The concept of *bandgap* stems directly from the sampling theorem which requires that a sequential measurement (e.g. of the voltage) was performed at least at twice of the maximal frequency of signal components (also called the Nyquist frequency), without additional assumption on their occurrence in time. Consequently, the bandwidth of discrete signal representation is being fully engaged in short time intervals only, while beyond these intervals it is overestimated and its redundant part does not carry components originated from the signal source. A bandgap occasionally appears between the variable instantaneous bandwidth of the signal the constant Nyquist frequency. It represents the noise component only. Time intervals with overestimated sampling and thus with the bandgap can be identified and localized by automatic detection of signal components provided they have a specific, a priori known limits of bandwidth. The existence of bandgap may be employed for accurate noise estimation [1], bit-accurate compression [2] or watermarking with supplementary data [3]. The latter case is presented in this paper.

The concept of bandgap is also hidden in image processing and used for compressed storage of images with smooth or texture-like regions detected. These parts are then efficiently represented with various techniques (e.g. multiresolution decomposition [4], [5]) without perceptible loss of quality. Digital images are well explored towards supplementary data embedment including steganography, secret sharing (e.g. [6], [7], [8], [9]) and encapsulating of other information such as in DICOM standard for medical images [10], [11], [12]. However, images due to their rigid structure (resolution, definition and frame rate) can be considered as packets and will not be discussed here.

II. Methods

A. General Case

A constant-bandwidth analog signal fills the throughput of transmission channel completely when the sampling frequency exactly matches the double of its bandwidth. This assumption is impractical for non-stationary signals and technical measuring systems overestimate the necessary throughput in order to avoid the aliasing. When seamless digital transmission is used, the constant-throughput channel is continuously available. Otherwise the signal is embedded in data packets and travel to the destination accordingly to a specific routing protocol. This allows for more economic usage of the channel, however the price for occasional excesses of channel throughput or transmission breaks is possible data delay.

This scientific work is supported by the AGH University of Science and Technology in year 2018 as a research project No. 11.11.120.612.

Piotr Augustyniak is with the AGH-University of Science and Technology 30, Mickiewicz Ave, 30-059 Krakow, Poland; (e-mail: august@agh.edu.pl).

.

In multidimensional unimodal measurement setups all signals are of the same nature and are considered as equally important. However in multimodal setups, which is often the case when extending the context of measured data, signals of different nature are usually captured at their specific frequencies and can be characterized by attributes of importance or immunity to delay. In this case adding a new measurement variable requires either a separate transmission/storage channel either extended data structures, possibly incompatible with precedent records. That is where watermarking technique is proposed to provide additional data containers of adjustable size, purpose and access privileges.

In the general case, we assume there is a digital signal (unimodal in case it is multidimensional) being a primary output of the considered measurement and imposing the throughput of the transmission channel by its peak bandwidth. To go beyond a very general data packet transmission, let us assume that this signal is time-critical i.e. the recipient does not accept delay. Later in this paper, we refer to this signal as the *carrier*. If the carrier shows temporal variations in bandwidth, the throughput of the channel is locally overestimated, the bandgap appears and thus the channel could accommodate more data.

Detection of these variations and resulting setup of supplementary data containers requires signal-specific research of expected local bandwidth. This important point falls out of the scope of this paper, we simply assume that the local bandwidth function is known and can be synchronized to the carrier with use of easily detectable signal landmarks.

We also assume there exist a supplementary digital data stream that is not time critical and thus suitable for packet transmission. This signal stems from auxiliary measurement (e.g. giving a context to the primary output) and is referred to as the *supplement*. In case of multiple such signals they can fit in interleaving data-tagged packets, spread in different channels of a multidimensional carrier, or have been aggregated in other way beforehand.

Two simplest approaches assume either a synchronous transmission of the carrier and the supplement with channels adjusted to their individual peak bandwidth (this can also be done in a single channel with signal modulation, but still needs a throughput being sum of individual peak bandwidth values), or a sequential transmission of both streams followed by synchronization (chopping signals in strips of constant duration prepares them to rigid structure of packets). The data integration process proposed in this paper assumes using the channel of carrier-related throughput and embedding the supplement packets in the bandgap whenever possible. In case the bandgap was too narrow to host the supplement synchronously to the carrier, the supplement is delayed. Beyond the point where the total data volume transmitted in given time equals the throughput of the channel, supplement delays cumulate and requires extension of the transmission time. In practice, this limitation occurs from lower data volumes due to the uncertainty of carrier's bandwidth variability and safety margin to be kept in order to avoid interference.

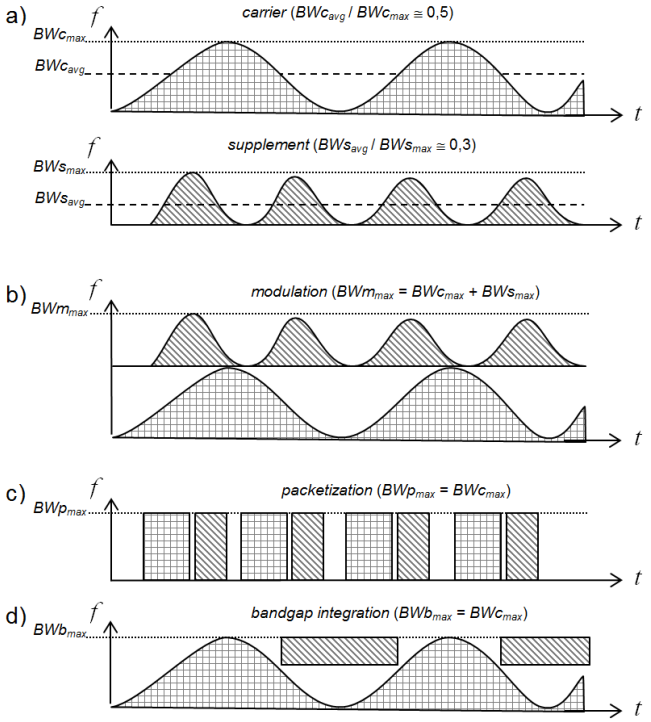

Fig 1. Methods of combining two data streams: a) separate carrier and supplement, b) modulation, c) packetization, d) bandgap integration.

B. Electrocardiogram case

Without loss of generality we focus on the digital electrocardiogram as the carrier. The ECG is an example of signal with variable instantaneous bandwidth, well known limitations on components' coincidence, and easy for a reliable segmentation thanks to algorithms engineered for the purpose of medical diagnostics [13]. The occurrence of various bandlimited components is more or less foreseeable, allowing for prediction of instantaneous bandwidth of the signal based on detection of these particular components. Since the bandgap does not contain components originating from the measured source, it is expected that replacing noise with the meaningful component of similar statistics preserves all diagnostic features, even if watermarked carrier is not bit-accurate to its clean counterpart.

With the growth of telemedicine the issue of patient's privacy and confidentiality protection is constantly stressed. According to Health Insurance Portability and Accountability Act (HIPAA) [14] sensitive data must be accessed by the authorized persons only. The information must also be kept confidential within transmission and storage equipment (e.g. hospital servers). This justifies a need for techniques in which sensitive information are hidden inside a host data without causing noticeable changes in the host data.

As telemedicine broadens its scope, additional measurements are often expected to accompany the principal data stream in order to shed light to distant measurement

conditions or to give a context for data interpretation. Supplementary data require additional transmission channels and storage structures which produces increased costs, impedes backward compatibility of records and increases a risk of accidental desynchronization [15]. Incorporating the supplementary data into biosignal's bandgap is then an interesting alternative without flaws mentioned above. Moreover, the proposed methodology of data fusion does not depend on the source or nature of the supplementary data. Additional signals, remote interpretation results, demographic or drug details, etc. may all be mixed in the supplementary data stream.

Seganography employing biosignals as data carrier was investigated in several papers published in the last decade [16], [17], [18], [19], [20], [3]. Recently, Jero and Ramu [21] suggested employing curvelets-based transform to hide valuable patient information into ECG signal and to adaptively select the location for watermarks. The secret information is coded into coefficients close to zero in the high-frequency sub-band. Wang et al. [22] has proposed yet another scheme based on unified embedding-scrambling method. This approach guarantees the security of secret information and the high quality of retrieved ECG signal. Finally, Dey et al. [23] provide a comprehensive review of different watermarking approaches in context of biomedical signal processing including recent applications and challenges.

In [24], a reversible error-correcting-coding strategy has been applied to transform digital signal into a bit-stream. This approach enable to pass a secret information using Hamming code, and it is fully blind and reversible technique. Liji et al. [25] proposed integer-to-integer wavelet transform to avoid truncation of the floating point values of the coefficients that may results in a loss of information using forward/inverse transformations. Other multi-scale object representation techniques were reported as suitable to store secret information.

Adaptive fitting of different data streams into a limited-throughput transmission channel has been widely studied and successfully implemented for packet-wrapped data [26]. In case of discrete signals a constant parameter (amplitude, frequency, phase etc.) modulation is used for splitting the throughput of the transport media accordingly to the maximum bandwidth of the signals [27]. Although several papers report the research on ECG watermarking, the proposals are mainly addressed to patient data protection or ECG content scrambling. Consequently two different approaches to the coding and decoding techniques are:

- coding makes the watermarked signal illegible and decoding restores bit accurate copies of both the carrier and the supplement;
- coding preserves the diagnostability of the watermarked carrier (i.e. although not bit-accurate it yields the same medical findings), decoding restores a bit-accurate copy of the supplement only.

We follow the later approach according to the idea of steganography. The ordinary reader (human expert or automatic interpretive software in case of ECG) is not aware about the existence of supplementary information and reads the basic but fully featured message. The privileged reader detects the auxiliary data packets and accesses the extended message. The meaning of the basic message and the basic part of extended message are thus identical.

III. The Integration Algorithm for ECG Carrier

A. Signal landmarks

The ECG is a quasi-periodic signal produced by three main electrical phenomena in the heart cycle of distinct cell activity (depolarization, repolarization) of different dynamics and by the conducting tissue (atria and ventricles). For the reasons of physiological difference, the maximum velocity of these phenomena and thus the local bandwidth of resulting signal depends on the relative progress of the heart cycle. The heart activity is represented by ECG waves separated and recognized by human expert or interpretive software. The history of software for cardiology dates back to 1967 and a huge experience allows for millisecond-precise delineation in case of best methods [28] [29]. These two reasons justify the selection of wave border points as landmarks in the ECG signal. Their order of occurrence in the heart cycle is: P-onset, P-end, QRS-onset, QRS-end and T-end. In specific cases P wave may not be present. The T-end point is relatively most difficult for calculation.

Moreover, we need a fiducial point easily detectable in both clean and watermarked carriers, where the positions of data container and data description are referred to. In case of the ECG, the R-wave maximum lying between QRS-onset and QRS-end was selected as optimal fiducial point.

B. Bandgap studies

To develop the concept of bandgap coding we need the local bandwidth of the signal to be a priori known at acceptable level of confidence and represented by detectable signal landmarks with acceptable reliability. In case of the electrocardiogram, three different methods were studied in our previous work to determine the local bandwidth and to attribute it to the P, QRS and T wave borders (fig. 2). Convergence of these methods was found sufficiently convincing to make the standardized bandwidth widely accepted.

First method [30] consists in separating waves in signals from various patients and analyzing the spectra of concatenated data series. A more accurate research used time-scale analysis and revealed even intra-wave variations of spectral contents.

Second method [31] relies on distortion of the ECG parameters and quality drop in result of local data canceling. The wavelet representation of the ECG was randomly altered in given range of time and scale and the reconstructed signal was interpreted again. The resulting difference of the parameters was evaluated in terms of possible degradation of

the final diagnosis. Since the only variable was placement of the signal alteration zone respective to the landmarks, we defined the 'local susceptibility' as a parameter estimating concentration of medically important information.

Third method [32] uses the analysis of expert scanpaths to indicate the most important sections of the electrocardiogram. With no assumption about the background physiology of the heart, we analyzed the distribution of gaze focus points and perceptual strategy from the experienced cardiologists to discreetly extract their knowledge gathered with years of clinical practice.

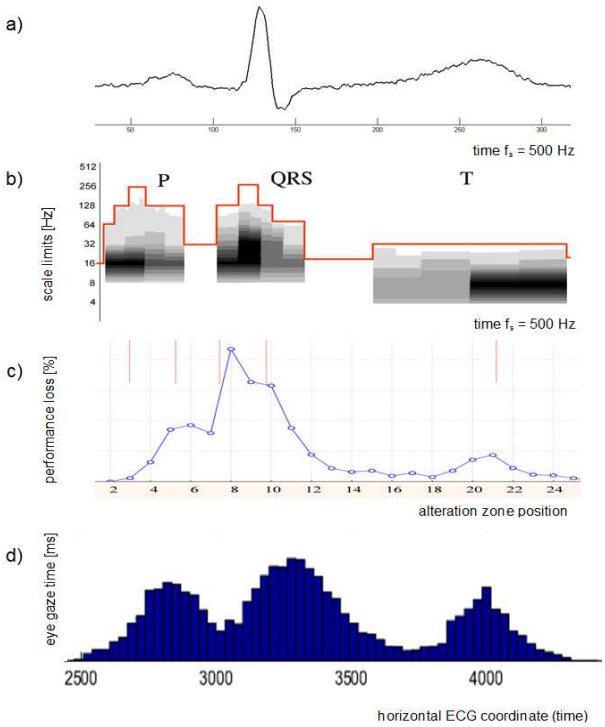

Fig. 2 Outcomes of the ECG local bandwidth studies a) the ECG (MIT-BIH file 100), b) analysis of the spectra of separate waves [30], c) analysis of influence from signal alteration zone position to diagnostic performance [31], d) analysis of experts scanpath distribution [32].

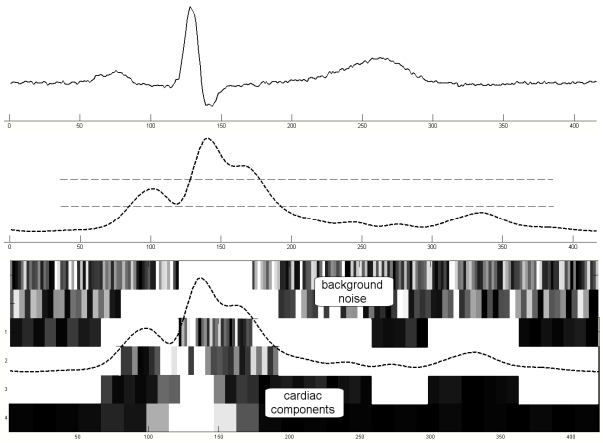

Fig. 3. Use of the standardized ECG local bandwidth function to separate cardiac and noise components in time-scale domain

These three experiments lead to the conclusion expressed by a standardized time function representing the expected bandwidth of the ECG relative to the landmarks (fig. 3). These landmarks are essential part of the result since they are necessary for time-stretching of the standard bandwidth in calculations of the value of bandwidth expected at a given point of a real signal.

C. *Scaling the bandwidth estimate*

In a wide range of quasi-periodical signals such as the ECG, the standardized instantaneous bandwidth requires a scaling transform that projects its general pattern to the actual strip of signal. Since in case of the ECG the bandwidth was defined relative to the wave borders, the bandwidth was scaled separately for each heart beat and wave border points were scaling-invariant.

For each heart neat the wave border points has been calculated with use of standard medical-grade algorithm, description of which may be found elsewhere. We used a modified Martinez algorithm [13] which shows one of the best available performance, but advantageously the calculations are performed in time-scale domain.

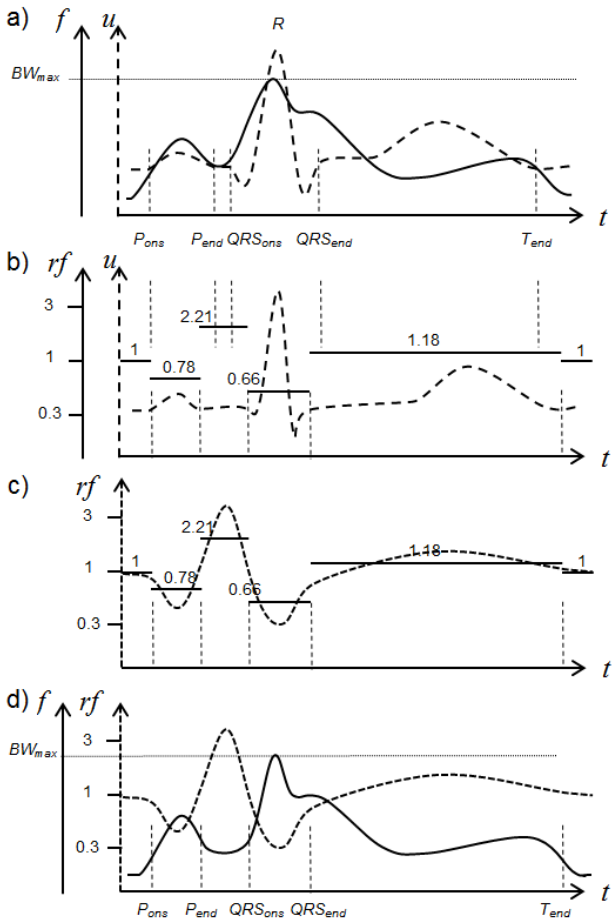

Fig 4. Steps of adaptation of standard ECG bandwidth to the landmarks of ongoing ECG signal; a) standardized instantaneous bandwidth with landmarks, b) stepwise resampling factor (*rf*) based on interval ratio, c) interpolated resampling factor, d) instantaneous bandwidth scaled to the new landmarks.

Scaling procedure has been implemented as dynamic resampling in three steps (fig. 4):

1. the for each consecutive interval a resampling factor is calculated so as to compensate for different length of corresponding sections in ongoing ECG signal and standardized bandwidth
2. consecutive values of local resampling factor are extrapolated to a discrete time function and interpolated with cubic splines with nodes falling exactly in border points.
3. the standardized bandwidth function is resampled with splines interpolation according to the local resampling value and considered as expected bandwidth of the ongoing ECG.

Since the wave border points are commonly determined for all simultaneous ECG leads in a multilead signal, expected bandwidth estimate is common for all these channels.

D. Supplement coding scheme

The supplement coding consists of three principal procedures.

First, the parameters of data components are determined based on local ECG properties: S-P distance and noise level. The length of the container extends from the QRS-end to P-onset points of the subsequent evolution with safety margins of ca. 60 ms. The margin length was selected accordingly to the temporal energy decay of the mother wavelet applied (db5) to assure low interference of the supplement with high frequency components of the carrier expected in P-onset to QRS-end section. The data container area is located in the first scale of time-scale ECG representation. The noise level is then measured in the container area and determines the coding bit depth (i.e. number of bits per sample, further referred to as CBD) of the supplement storage as $\lceil \log_2 v_{p\text{-}p} \rceil$. This preparation step is required for preparing of the supplement so as it closely mimics the original noise statistics (fig. 5). The value of CBD determines the data capacity of each individual noise container. In practice the length of S-P section varies from beat to beat and the noise level also from channel to channel.

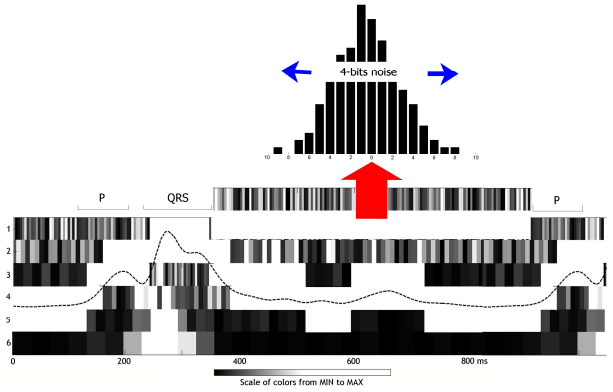

Fig. 5 Determining coding bit depth (CBD) based on the bandgap noise statistics.

The supplement data stream is then tailored in the packet of length and CBD fitting to the destination data container. Remaining part of the supplement data is queued for encoding in next available container. The supplement data directly replace time-scale values in the container area (fig. 6a). If there is not enough supplement data to fill the space available in the container, the actual length of the container is updated.

The final step consists in encoding the container description. Unlike the data, the container description is made with a single bit (i.e. an LSB coding [19]) in a fixed structure in the second scale of time-scale ECG representation (fig. 6b). This structure consists of 18 bits: the beginning with respect of precedent R peak (6 bits), the length (9 bits), and maximum CBD (3 bits). It begins at the point delayed by 100 ms from the R-peak and lasts for 144 ms which is short enough to avoid interference with high frequency components of the P wave from next heart beat. Such arbitrary selection guarantees the independence of the description field and the ECG content and simplifies the decoding process.

When necessary, the description may be integrated with:

- encryption key in case of ciphered supplement,
- mother wavelet code,
- additional code tagging the supplement content.

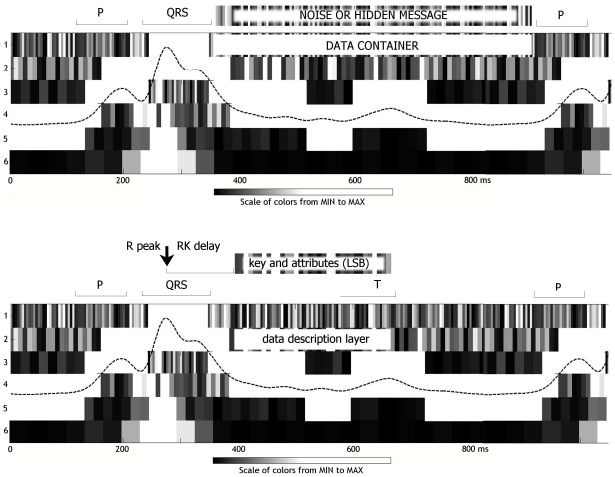

Fig. 6 Encoding a) the supplement in the data container, b) the data container description

All manipulations to the carrier are made in its time-scale representation and thus embraced by two complementary steps of forward and reverse wavelet transform (fig. 7).

E. Supplement decoding scheme

Since the watermarked carrier preserves the consistence of the basic message (i.e. all diagnostic features in case of the ECG), it is not modified in the decoding scheme. However, extracting of the data container description and subsequently the supplement data requires the time-scale representation of watermarked carrier, which is calculated with the wavelet transform identical in terms of wavelet type and order to those used for encoding.

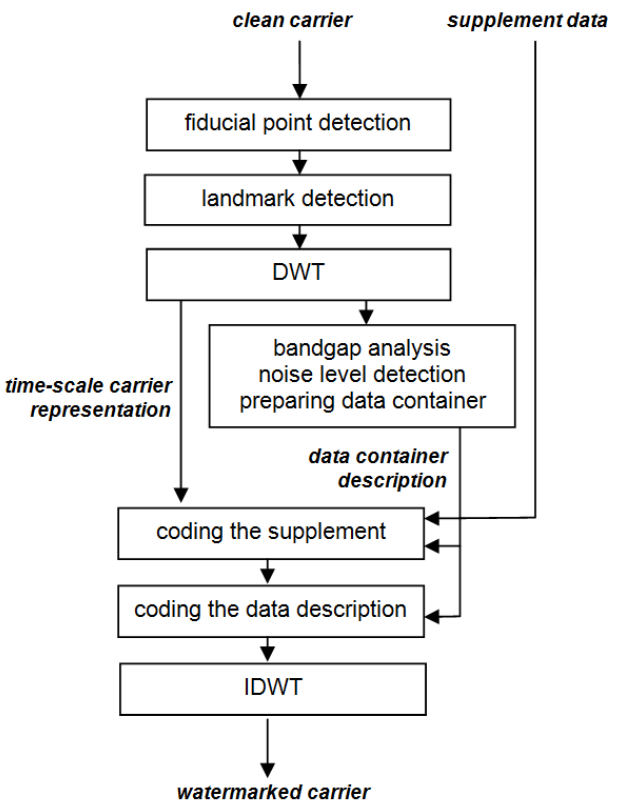

Fig. 7. Time-scale domain data watermarking scheme

The first bit of data description structure is located at a fixed distance to the fiducial point, and requires the decoding scheme to include a R-peak detection procedure. Detection accuracy has to be superior than the half of length of time-frequency atom in the second scale (i.e. double of the sampling interval). Once read, the data description points at the beginning of data container and provides information on the length of the data and CBD, what allows for unambiguous extraction of the supplement content (fig. 8). In case of additional data ciphering, the data description, the data itself or both can be scrambled with appropriate technique.

F. Transparency test

The watermarking transparency test proves whether the basic message (the original carrier) and the basic part of extended message (watermarked carrier) yield the same medical findings. For this purpose we applied the industry standard IEC 60601-2-51 on required performance of interpretive electrocardiographs [33] and the certified interpretive ECG machine allowing for external SCP signal processing (MTrace M4Medical). The standard specifies a subset of CSE reference files [34] and the acceptable statistics of differences between measured and reference values (length of P, PQ, QRS and QT segments). The CSE Multilead Dataset 3 consists of 125 ECG and VCG signals (f_s = 500 Hz, 12 bit/10mV) each of 10 s duration and multicenter manual and machine reference interpretation results.

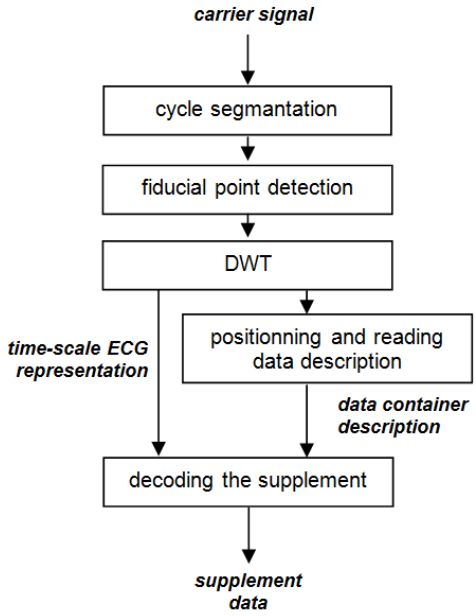

Fig. 8. Time-scale domain supplement decoding scheme

The watermarking was considered transparent if results of both the original and watermarked ECG carrier fall within the acceptance margin. The test was performed for different watermarking schemes (mother wavelet, wavelet order) in order to minimize the supplement interference with the ECG carrier.

Table 1 presents the results of average wave measurement accuracy calculated accordingly to IEC 60601-2-51 for original and watermarked ECG signals (db5 wavelet).

TABLE I. ACCURACY OF WAVE MEASUREMENT FOR ORIGINAL CSE SIGNALS AND THEIR VERSIONS INCORPORATING THE EXERCISE DATA [MS]

ECG Section	Original Signal		Watermarked Signal		IEC Allowed Tolerance	
	mean	*std*	*mean*	*std*	*mean*	*std*
P	±4.3	3.3	±4.5	3.3	±10	15
QRS	±2.1	1.7	±2.1	2.4	±10	10
P-Q	±3.8	4.7	±4.0	5.1	±10	10
Q-T	±11.3	7.3	±11.8	10.8	±25	30

Temporal parameters, based on distances between borders of consecutive waves, are fundamental for medical findings and the required precision of the calculations is specified by international standard regulations (see [33]). Therefore the results presented in Table 1 prove the medical equivalence of the original ECG (a clean carrier) with its counterpart hosting the supplement.

As the supplement data container occupies first scale in time intervals simultaneous to the T-wave, the duration of Q-T section is probably the most exposed to possible changes due to watermarking. To prove the necessity for continuous noise tracking, we modified the impact of noise level measurement by artificially adding bits to the resulting supplement CBD.

TABLE II. ACCURACY OF Q-T INTERVAL MEASUREMENT FOR WATERMARKED CSE SIGNALS WITH MODIFIED NOISE IMPACT [MS] VALUES EXCEEDING THE IEC TOLERANCE ARE PRINTED IN BOLDFACE

Coding Bit Depth vs. Noise Level (bits)	Difference of Q-T Section Length	
	mean	std
-2	±23.1	**37.4**
-1	±14.3	21.5
0	±11.8	10.8
1	**±33.4**	**50.8**
2	**±67.8**	**91.3**

The results displayed in Table 2 proved that accurate noise level tracking is necessary for correct modulation of the CBD. Consequently, the statistics of embedded motion data mimic the properties of intrinsic noise and the watermarking process does not alter the medical interpretation of the host record. Table 2 also shows that overestimating the noise level slightly increases the QT-length calculation error, while the opposite alters the ECG record significantly making it unusable.

IV. APPLICATION CASES

Three cases of prototype application are presented in this section. They employ a common background of ECG watermarking and showcase the applicability of the method for integrating of patient data, carrying data of extended sampling, or additional exercise data from homemade measurements.

A. Integrating patient data

As watermarking is usually related to data integration and steganography, our first study concerned including of patient sensitive information into the signal [35]. We coded a regular alphanumeric message equivalent to patient demographic data or plain text diagnostic result. Additionally, the record (up to 78 characters per heartbeat) may be recovered or not, depending only on reader's privileges.

We used the commercial IEC-certified interpretation software to assess the influence of supplementary digital data to the accuracy of the wave's delimitation. Main assessment of the method was made in diagnostic parameters domain (Table 3), Additionally differences between original and watermarked carriers were measured with percent root-mean-square difference (PRD).

Since the level of intrinsic noise in CSE database signals falls slightly above 10 μV, and the signal resolution is 0.25 μV/LSB, CBD of 5 bits doesn't deteriorate the signal significantly. From the IEC recommendation viewpoint, the acceptable values of standard deviations for global durations and intervals are not exceeded. In case of larger densities (i.e. CBD values), the supplement data are less similar to the noise statistics and consequently:

- are more pronounced in statistical parameters and
- systematically interfere with cardiac components and degrade the diagnostic result.

TABLE III. STANDARD DEVIATIONS FOR GLOBAL DURATIONS AND INTERVALS FOR WATERMARKED ECGS (ACCORDINGLY TO IEC) AND AVERAGE PRD VALUES

Coding Bit Depth [bits]	deviation of interval duration [ms]				PRD [%]
	P	PQ	QRS	QT	
0 (orig. ECG)	4.51	3.93	3.55	9.82	0
1 (0.5 μV)	4.55	3.79	4.16	10.5	0.03
2 (1.0 μV)	4.81	3.98	4.39	12.3	0.06
3 (2.0 μV)	6.93	4.12	4.89	15.1	0.13
4 (4.0 μV)	9.11	4.33	6.16	18.9	0.27
5 (8.0 μV)	12.5	4.52	8.88	27.1	0.51

Due to the adaptation of hidden data container to local ECG properties, its capacity may be only roughly determined. In the electrocardiogram sampled at 500 Hz with amplitude resolution of 0.25 μV/LSB (where 16 bits correspond to ±8.2 mV) representing a Normal Sinus Rhythm of 72 bpm and average P-QRS duration of 250 ms, the CBD of 5 bits represent the data stream for hidden message of 725 bps (i.e. 9.1% of the carrier ECG data rate).

Three features of the proposed patient data integration method are worth highlighting:

- the method doesn't assume a uniform coding of a hidden message, but adapts the container size and CBD to best mimic the noise present in the original electrocardiogram,
- each heart beat constitutes an independent data container - by using various combination of RK distance, and key pattern, messages hidden in the record may be selectively accessible to the users of various privileges,
- the hidden message coding doesn't affect the most informative (i.e. medically important) sections in the electrocardiogram (see tab. 1 column PQ).

B. Extended sampling

Standard bandwidth of the ECG is estimated to 250 Hz, what makes the sampling frequency of 500 Hz appropriate in most cases. However in some diseases pathological high frequency components may occur (e.g. ventricular late potentials) or for some measurements the measurement precision is not sufficient (e.g. T-wave alternans). When such necessity was known beforehand, a high-resolution ECG was captured with a recorder with extended sampling parameters (typically: 4kHz, 16 bit), also known as High Resolution ECG.

Despite limited capacity, the extra storage space in supplement data containers can accommodate high frequency details of the signal. Encoding these information allows privileged users for a high precision analysis, while regular users with an access to standard resolution signal are still able to correctly calculate essential diagnostic parameters. The privileges assigned may depend on software manufacturer or health care provider and any available symmetric-key or asymmetric-key cryptographic algorithms may be used.

In the proposed prototype [36] the ECG signal is originally

acquired with a four-fold oversampling (i.e. f_s = 2 kHz), therefore the scales are indexed as: {-1, 0, 1, 2, etc.}. The encoding algorithm starts with two steps typical for medical interpretation: heartbeat detection and delimitation of selected wave borders. Next, the time-scale transform is performed and the content of the 1-st scale is investigated in the S-P section for noise estimate as described in 3.4

Next step consists of analysis of the content of the -1st and 0th scales in specified region of interest (ROI). The coefficients are decorrelated using a Discrete Cosine Transform [37] that sorts them in the order of decreasing energy. If the total volume of complementary details exceeds the capacity of data container, least significant components of the details are truncated causing minimal distortion of the details.

The extended sampling representation is then coded using selected CBD value and replaces lowest significant bits of the consecutive time-frequency coefficients in 1st scale as the supplement content (fig. 9). The public part of encryption key, position of first coefficient of the 1st scale, the actual data container length and CBD are stored as container description are encoded in the 2nd scale of host ECG using LSB method.

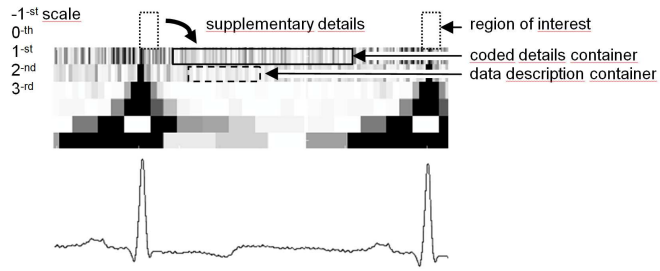

Fig. 9. Encoding the electrocardiogram details in the host record's bandgap [36]

The proposed algorithm was tested accordingly to the industry standard with use of files from CSE Multilead Dataset 3 [34]. The details were artificially added 500 Hz triangular waves limited to the ROI with the amplitude of 6.25% of the QRS voltage. The size of ROI varies from 10 to 50 ms, what corresponds to details volume of 120 to 600 bits per heartbeat. Depending on applied CBD (in the range of 1 to 5 bits/sample), the expected storage capacity at 72 bpm NSR is 180 to 900 bits per heartbeat.

We calculated the PRD values for pairs of signals:

- original and watermarked ECG carriers (E_{PRD}),
- original and decoded detail signals (D_{PRD}).

When the coding uses high CBD values, it fails to mimic the statistic properties of the noise and causes distortions in the electrocardiogram (E_{PRD}). On the other hand, using low CBD limits the size of hidden data container (which additionally varies with the ECG content), thus the prioritized sequence of details has to be truncated accordingly causing detail signal distortions (D_{PRD}). Main results of testing are distortion values measured as D_{PRD} and E_{PRD} (Tab. 4).

TABLE IV. AVERAGE COMPLEMENTARY DETAILS (D_{PRD}) AND ECG SIGNAL (E_{PRD}) DISTORTION VALUES FOR CODING BIT DEPTH RANGING FROM 1 TO 5 BITS PER SAMPLE.

Coding Bit Depth [bits]	D_{PRD} ROI duration [ms]			E_{PRD} [%]
	10	25	50	
1 (0.5 μV)	0	0.41	1.16	0.03
2 (1.0 μV)	0	0.14	0.59	0.06
3 (2.0 μV)	0	0.05	0.28	0.13
4 (4.0 μV)	0	0	0.07	0.27
5 (8.0 μV)	0	0	0	0.51

First column of Table 4 presents CBD values and corresponding noise voltages. While E_{PRD} values only depends on the CBD, the D_{PRD} is a result of truncating the prioritized chain of detail coefficients and additionally depends on the ROI duration.

C. Homemade equivalent of exercise test

Cardiac ischemia is currently found a primary cause of death in developed countries and thus constitutes an important individual risk factor as well as an immense public health problem. Unfortunately, reliable ischemia markers require biochemical analysis of blood and the exercise test, although more practical, raises the risk of acute infarct and thus requires a supervision in the cardiologist's office. This test consists in exposing the patient to the controlled physical load (with a treadmill or cycle ergometer), modulated accordingly to a given protocol and recording basic physiological parameters (heart rate, blood pressure and possible ischemia symptoms). Deficient oxygenation of the heart manifests itself by changes in early repolarization stage and can be detected based on measurements of the ST segment in the electrocardiogram [38]. The results of ST-segment amplitude and slope crossing are compared to arbitrarily given thresholds and excessing values trigger alerts. Unfortunately the unified approach weaknesses the sensitivity of the method and the inconvenience related to regular exercise testing significantly decreases the participation of patients.

Designing a ubiquitous equivalent for exercise test requires to eliminate the risk of exceeding the load and complexity of the measurement. This may be achieved with reducing the load to everyday living activities and moving the test from the cardiologist's office to patients' homes [39]. Unfortunately, in order to correctly interpret the possible ST changes, the method requires measurement of instantaneous load and blood pressure along with the ECG.

In home monitoring condition, physical load required by everyday living activities replaces a standardized load control protocol, with acceptably inferior accuracy. With the continuous ECG record and a supplement data from set of three accelerometers mounted on wrist, waist and ankle and appropriately individual-calibrated biomechanical model it is possible to approximate the power exercised in everyday living conditions [40]. Small battery-operated and Bluetooth-

enabled accelerometers can easily be embedded in clothes (e.g. watch, belt and shoe) and communicate as nodes of a wireless sensor network under the supervision of ECG recorder. Accordingly to [41] it is sufficient to sample accelerometer data at the rate of 15 Hz and with resolution of 12 bits, thus three 3-axial devices yield a constant bit stream of 1620 bps.

The sensor set used in homemade exercise test is presented in Fig. 10. The wrist accelerometer was attached to the watch strap on the left hand, the ankle accelerometer was attached to the elastic strap on the top of left foot sock. The third accelerometer, instead of waist was mounted in the chest front together with one of the ECG capturing electrodes.

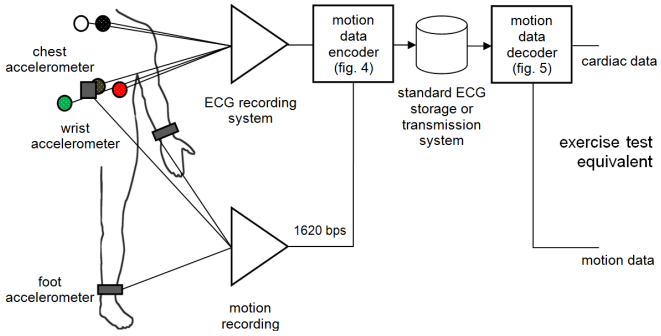

Fig. 10. Block diagram of the home exercise monitoring system using standard ECG channels for hosting supplementary accelerometer data.

In the experiment with 17 original exercise test records, the watermarked signals were returned to the stress-test analysis procedure to calculate differences in elevation/depression and the slope of the S-T segment. These parameters are indicative for coronary ischemia, transmural myocardial infarction, subendocardial myocardial infarction or other serious heart failures.

The ST elevation/depression is measured in microvolts as the difference of average values of ECG signal samples between ST-segment border points and average values of ECG signal samples on the baseline preceding the QRS complex. A threshold of 100 μV is commonly used to check whether the measured elevation of S-T slope indicates the ischemia. The ST-segment slope is measured as the sign of slope coefficient of the straight line best fitted to the ECG signal samples between ST-segment border points. The slope is either positive (rising upwards) or negative (falling downwards).

TABLE V. DIFFERENCE OF ISCHEMIA-RELATED PARAMETERS OF S-T SEGMENT IN REAL STRESS TEST ELECTROCARDIOGRAMS DUE TO WATERMARKING

S-T Parameter	Parameter Difference	
	mean	***std***
elevation/depression [μV]	±15.7	41.0
threshold mismatch cases	2	
slope coefficient	±0.157	0.203
slope sign mismatch cases	1	

Results of S-T segment measurement in original and watermarked exercise cardiograms are displayed in Table 5.

The experiment with real stress test ECG's revealed a very limited influence of embedded data to the interpretation result. ST-segment parameters, principal in this test, are expressed in amplitude units and therefore replacing the time-scale coefficients related to noise with auxiliary data causes measurement errors. The errors, however are not significant, in two cases (out of the total 17) the excess of the threshold amplitude was detected differently in corresponding original and watermarked ECGs. The value of slope coefficient also shows little difference and in one single case the slope was reported from watermarked signal as positive instead of negative that was in case of the original.

V. DISCUSSION AND CONCLUSIONS

The proposed method inherited advantages of few previously published steganography algorithms, however detection and usage of the instantaneous bandwidth of a biological signal (taking the ECG as an example) and considering a non-uniform distribution of its diagnostic relevance is a novelty in digital signal processing.

Three presented examples of ECG-related application showed that in case of a signal consisting of bandlimited easily detectable components, the detection of the bandgap and estimation of its properties is confident enough to guarantee efficient and transparent integration of supplementary data. In all examples the original throughput of the transmission channel and data storage structures were maintained and the ECG carrier did not experience delay.

To go beyond the ECG-related examples and make the main result applicable for a broad range of signals acquired in biology and industry, a general framework of measurement and data transmission is needed. It should include:

- generalization of rules for bandgap detection in various signals,
- providing a set of methods for data containers design and implementing exemplary containers in several variants for supplementary data coding,
- validation of effectiveness and transparency of the coding process for different variants of containers and volumes of supplementary data stream and various content of the carrier.

REFERENCES

[1] P. Augustyniak " Time-frequency modelling and discrimination of noise in the electrocardiogram," *Physiological Measurements* 24(3), 2003, 753-767

[2] K. Duda, P. Turcza and T. P. Zielinski, "Lossless ECG compression with lifting wavelet transform," IMTC 2001. Proceedings of the 18th IEEE Instrumentation and Measurement Technology Conference. Rediscovering Measurement in the Age of Informatics, Budapest, 2001, pp. 640-644 vol.1.

[3] K.-K.Tseng, X. He, W.-M. Kung, S.-T. Chen, M. Liao, H.-Y. Huang, "Wavelet-Based Watermarking and Compression for ECG Signals with Verification Evaluation," Sensors 2014, 14, 3721-3736

[4] Chiou-Ting Hsu, Ja-Ling Wu " Multiresolution Watermarking for Digital Images," IEEE Transactions on Circuits and Systems—II: Analog and digital signal processing, 45(8), 1998, pp. 1097-1101

[5] M.N. Do, M. Vetterli, "The contourlet transform: an efficient directional multiresolution image representation," IEEE Transactions on Image Processing (Volume: 14, Issue: 12, Dec. 2005, pp. 2091 – 2106
[6] Chin-Chen Chang, Pei-Yu Lin, Chi-Shiang Chan, "Secret Image Sharing with Reversible Steganography," 2009 International Conference on Computational Intelligence and Natural Computing. DOI 10.1109/CINC.2009.249
[7] M. Ulutas, R. Yazıcı, V.V. Nabiyev, G. Ulutas "(2,2)-Secret Sharing Scheme with Improved Share Randomness," 23rd International Symposium on Computer and Information Sciences, 2008. ISCIS '0, DOI: 10.1109/ISCIS.2008.4717857
[8] P. Li, P. Ma, X. Su "Image secret sharing and hiding with authentication," 2010 First International Conference on Pervasive Computing, Signal Processing and Applications, DOI 10.1109/PCSPA.2010.10
[9] C.-N. Yang, T.-S. Chen "An Image Secret Sharing Scheme with the Capability of Previvewing the Secret Image," 2007 IEEE International Conference on Multimedia and Expo, 2007, pp. 1535 - 1538
[10] J. M. Zain, L.P Baldwin, M. Clarke "Reversible watermarking for authentication of DICOM images," Conf Proc IEEE Eng Med Biol Soc. 2004;5:3237-40.
[11] G. Coatrieux, L. Lecornu, Ch. Roux, B. Sankur, A Review of Image Watermarking Applications in Healthcare, 28th Annual International Conference of the IEEE Engineering in Medicine and Biology Society, 2006. EMBS '06. DOI: 10.1109/IEMBS.2006.259305
[12] Malay Kumar Kundu, Sudeb Das, "Lossless ROI Medical Image Watermarking Technique with Enhanced Security and High Payload Embedding," 2010 International Conference on Pattern Recognition, DOI 10.1109/ICPR.2010.360
[13] J.P. Martínez, R. Almeida, S. Olmos, A.P. Rocha, P. Laguna, "A wavelet-based ECG delineator: evaluation on standard databases," IEEE Trans. Biomed. Eng. 2004; 51:570–581
[14] W. Lee, C. Lee, "A cryptographic key management solution for HIPAA privacy/security regulations," IEEE Trans. Inf. Technol. Biomed. 2008, vol. 12, no. 1, pp. 34-41
[15] E. Kańtoch, D. Grochala, M. Kajor, "Bio-inspired topology of wearable sensor fusion for telemedical application," Artificial Intelligence and Soft Computing : 16th International Conference : ICAISC 2017 Zakopane, Poland, June 11–15, 2017, pp. 658–667
[16] P.K. Dilip, V.B. Raskar, "Survey Paper on Wavelet Based ECG Steganography," International Journal of Research in Engineering and Technology, Vol. 04 (03), 2015, pp. 165-169
[17] M. Engin, O. Cıdam, E.Z. Engin, "Wavelet Transformation Based Watermarking Technique for Human Electrocardiogram (ECG) ," Journal of Medical Systems 2005;29(6):589–594.
[18] S. Kaur, O. Frooq, R. Singhal, B.S. Ahuja, "Digital watermarking of ECG data for secure wireless communication," International Conference on Recent Trends in Information, Telecommunication and Computing, IEEE Computer Society, 2010.
[19] A. Ibaida, R. van Schyndel, "A low complexity high capacity ECG signal watermark for wearable sensor-net health monitoring system, Computing in Cardiology 2011;38:393-396, ISSN 0276-6574.
[20] I. Ayman, K. Ibrahim, "Wavelet-Based ECG Steganography for Protecting Patient Confidential Information in Point-of-Care Systems," IEEE Trans. Biomed. Eng. 2013, 60, 3322–3330
[21] S.E. Jero, P. Ramu, "Curvelets-based ECG steganography for data security," Electronics Letters 52.4, 2016, 283-285
[22] H. Wang, Z. Weiming, Y. Nenghai, "Protecting patient confidential information based on ECG reversible data hiding," Multimedia Tools and Applications 75.21, 2016, 13733-13747
[23] N. Dey et al. "Watermarking in Biomedical Signal Processing," [in:] Intelligent Techniques in Signal Processing for Multimedia Security. Springer International Publishing, 2017. 345-369.
[24] H.J. Shiu, B.S. Lin, C.H. Huang, P.Y. Chiang, C.L. Lei, "Preserving privacy of online digital physiological signals using blind and reversible steganography," Computer Methods and Programs in Biomedicine 2017, vol. 151, 159-170
[25] C.A. Liji, K.P. Indiradevi, K.A. Babu, "Integer-to-integer wavelet transform based ECG steganography for securing patient confidential information," Procedia Technology 2016, vol. 24, 1039-1047
[26] N.F. Mir, Computer and Communication Networks, 2nd Edition, Prentice Hall, 2014
[27] T.S. Rappaport, Wireless Communications: Principles and Practice, IEEE Press 1996
[28] N. Bayasi, T. Tekeste, H. Saleh, A. Khandoker, B. Mohammad, M. Ismail, "Adaptive technique for P and T wave delineation in electrocardiogram signals," 36th Annual International Conference of the IEEE Engineering in Medicine and Biology Society (EMBC), 2014 DOI: 10.1109/EMBC.2014.6943536
[29] A. Martínez, R. Alcaraz, J.J. Rieta, "Application of the phasor transform for automatic delineation of single-lead ECG fiducial points," Physiol. Meas. 2010; 31:1467–1485.
[30] P. Augustyniak "Moving Window Signal Concatenation for Spectral Analysis of ECG Waves," Computing in Cardiology 2010, pp. 665-668
[31] P. Augustyniak "Pursuit of the ECG Information Density by Data Cancelling in Time-Frequency Domain" – IFMBE Proc. vol. 2 2002, pp. 152-153
[32] R. Tadeusiewicz, P. Augustyniak, "Analysis of human eye movements during the plot inspection as a tool of assessment of local informative value of the 12-lead ECG," Biocybernetics and Biomedical Engineering 2007 vol. 27 number 1/2 pp. 169-176
[33] IEC 60601-2-51, Medical electrical equipment: Particular requirements for the safety, including essential performance, of ambulatory electrocardiographic systems. First edition 2003-02, International Electrotechnical Commission, Geneva, 2003
[34] J.L. Willems, P. Arnaud, J.H. van Bemmel et al. "A reference database for multilead electrocardiographic computer measurement programs," Journal of the American College of Cardiology, 6, 1313-1321, 1987
[35] P. Augustyniak "Analysis of ECG Bandwidth Gap as a Possible Carrier for Supplementary Digital Data," Computing in Cardiology 2012;39:73–76
[36] P. Augustyniak "Encoding the Electrocardiogram Details in the Host Record's Bandgap for Authorization-Dependent ECG Quality," Computing in Cardiology 2014, vol. 41, 465-468
[37] N. Ahmed, T. Natarajan, K.R. Rao, "Discrete cosine transform," *IEEE Trans. on Computers*, 1974, C–23, 90–93
[38] P. T. O'Gara, et al., "2013 ACCF/AHA Guideline for the Management of ST-Elevation Myocardial Infarction," Circulation. vol.127, 2013, pp. e362-e425
[39] [camcs18] P. Augustyniak, "Application of Watermarking Technique to Embedding Homemade Exercise Test Data into a Standard ECG Signal" International Conference on Applied Mathematics and Computer Science (ICAMCS 2018), Paris, France April 13-15, 2018.
[40] H. Ghasemzadeh and R. Jafari, "Physical movement monitoring using body sensor networks: A phonological approach to construct spatial decision trees," IEEE Transactions on Industrial Informatics 7 (1), 2011, pp. 66-77
[41] U. Maurer, A. Smailagic, D.P. Siewiorek and M. Deisher, "Activity recognition and monitoring using multiple sensors on different body positions. In: Wearable and Implantable Body Sensor Networks, International Workshop on BSN 2006. IEEE, pp. 4 pp.–116 doi: 10.1109/BSN.2006.6

Piotr Augustyniak graduated in 1989 in electronic engineering and received the PhD degree in electronics (1995, with honors) and the DSc (habilitation) in automatics (2004) all from the Electrical Engineering Department AGH-University of Science and Technology, Krakow. Since 1989, he has been working at the Automatics and Biomedical Engineering Department, as a Research Scientist, an Assistant Professor, an Associate Professor and since 2016 as a Full Professor. In years 2005-2012, he headed the Multidisciplinary School of Engineering in Biomedicine. For 11 years he has worked at Aspel SA, the Poland-biggest manufacturer of ECG equipment as a Research Enginee.

His scientific interests include hardware and software problems of biosignal processing. He published nine books on electrodiagnostic signal processing, over 230 journal and conference papers and was program committee member of numerous international conferences.

Prof. Augustyniak is member of the International Society of Electrocardiology and of the Computing in Cardiology Society. Recently he is Vice-president of Poland Section IEEE Signal Processing Society.